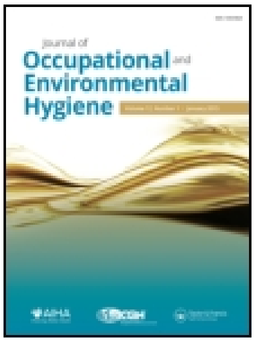

Taylor & Francis
Taylor & Francis Group

Journal of Occupational and Environmental Hygiene

ISSN: 1545-9624 (Print) 1545-9632 (Online) Journal homepage: http://www.tandfonline.com/loi/uoeh20

The effect of simulated air conditions on N95 filtering facepiece respirators performance

Joel A. Ramirez & Patrick T. O'Shaughnessy

To cite this article: Joel A. Ramirez & Patrick T. O'Shaughnessy (2016) The effect of simulated air conditions on N95 filtering facepiece respirators performance, Journal of Occupational and Environmental Hygiene, 13:7, 491-500, DOI: 10.1080/15459624.2016.1143950

To link to this article: http://dx.doi.org/10.1080/15459624.2016.1143950

Accepted author version posted online: 09 Feb 2016.
Published online: 26 Apr 2016.

JOURNAL OF OCCUPATIONAL AND ENVIRONMENTAL HYGIENE
2016, VOL. 13, NO. 7, 491–500
http://dx.doi.org/10.1080/15459624.2016.1143950

Taylor & Francis
Taylor & Francis Group

The effect of simulated air conditions on N95 filtering facepiece respirators performance

Joel A. Ramirez and Patrick T. O'Shaughnessy

Department of Occupational and Environmental Health, College of Public Health, The University of Iowa, Iowa City, Iowa

ABSTRACT
The objective of this study was to determine the effect of several simulated air environmental conditions on the particle penetration and the breathing resistance of two N95 filtering facepiece respirator (FFR) models. The particle penetration and breathing resistance of the respirators were evaluated in a test system developed to mimic inhalation and exhalation breathing while relative humidity and temperature were modified. Breathing resistance was measured over 120 min using a calibrated pressure transducer under four different temperature and relative humidity conditions without aerosol loading. Particle penetration was evaluated before and after the breathing resistance test at room conditions using a sodium chloride aerosol measured with a scanning mobility particle sizer. Results demonstrated that increasing relative humidity and lowering external temperature caused significant increases in breathing resistance ($p < 0.001$). However, these same conditions did not influence the penetration or most penetrating particle size of the tested FFRs. The increase in breathing resistance varied by FFR model suggesting that some FFR media are less influenced by high relative humidity.

KEYWORDS
Breathing resistance; cyclic flow; filtering facepiece respirators; particle penetration

Introduction

Filtering facepiece respirators (FFRs) are well-recognized personal protective equipment used by workers to provide protection against airborne particulates in a variety of occupational settings.[1] An estimated three million workers wear FFRs throughout the United States in an estimated 200,000 workplaces.[2] Agriculture, manufacturing, construction, and mining are some of the industries that use FFRs.[3] FFRs worn correctly will protect the wearer in many workplace settings and can prevent acute or chronic health symptoms to the wearer.

Particle removal efficiency and breathing resistance (BR) are the principal criteria for measuring FFR performance.[4] The National Personal Protective Technology Laboratory (NPPTL) of the National Institute for Occupational Safety and Health (NIOSH) certifies the filters associated with different respirator types using the method described in the Code of Federal Regulations (Title 42 CFR Part 84).[1] The filter of a N95 FFR, the most commonly used FFR, will remove at least 95% of particles in the air that the user is breathing. The NPPTL tests filter efficiency and BR in a laboratory setting where the variables of temperature (77°F), relative humidity (30%), and one-direction airflow (85 L/min) are controlled. FFRs are certified when the inhalation BR is less than 35 mm of H_2O and the exhalation BR is less than 25 mm of H_2O measured at constant one-direction airflow of 85 L/min.[5] However, FFR efficiency and BR can be affected by numerous conditions such as air velocity, particle diameter, fiber diameter, and humidity.[6–8] Furthermore, high humidity conditions where FFRs may be used, for example when power washing, can differ from the laboratory humidity conditions where FFRs are certified.

FFR filter efficiency and BR are measured by testing the filter with a constant high air flow from the outside to the inside of the FFR. However, when FFR users breathe air it moves in two directions, inhalation and exhalation flows, that follow a cyclic flow pattern.[6] Despite a large amount of research associated with evaluating FFRs, few studies have been conducted to determine FFR efficiency under cyclic flow.[7–10] Cho et al.[7] demonstrated that filter penetration decreased with increasing particle size (0.7–4 µm). Cho et al.[8] found that filter penetration was below 5% for the N95 respirators tested as required for that type of respirator. Eshbaugh et al.[9] found that particle capture efficiency decreased with an increase in air

CONTACT Patrick T. O'Shaughnessy patrick-oshaughnessy@uiowa.edu Department of Occupational and Environmental Health, College of Public Health, 100 CPHB, S320, Iowa City, IA 52242
Color versions of one or more of the figures in the article can be found online at www.tandfonline.com/uoeh.

flow rate. Grinshpun et al.[10] demonstrated that particles in the range between 0.04–1 μm penetrated the filter media less than 1% in one N95 FFR. However, these studies did not evaluate the effect of humidity on FFR performance. Therefore, it is not clear how humidity will affect efficiency and BR of FFRs under cyclic flow.

Various studies have been conducted to evaluate BR of FFRs.[11–14] Janssen[11] observed a statistically significant increase in BR when the FFR was challenged against cement dust, but below the pressure limit established by NIOSH.[10] Cho et al.[13] reported that BR increases faster when the filter was loaded with welding fume versus when loaded using NaCl aerosol in a laboratory setting. Cho and Yoon[14] observed a BR increase when filters were loaded with welding fume in a field setting. However, neither of these studies evaluated the effects of humidity on the BR of the FFRs. Only Roberge et al.[12] investigated the effect of exhaled moisture on BR of N95 FFRs. Under ambient conditions, a BR increase of 3% was observed. However, that study did not look at different humidity conditions upstream of the FFR. For example, air condensation will occur when air temperature outside the body is lower than the body temperature or when moisture is high.[15] Therefore, it is still not clear how ambient humidity will affect BR of FFRs.

Previous work has shown the effects of humidity on the efficiency across high efficiency particulate air (HEPA) filters.[16,17] Miguel[16] found that filter efficiency decreases as humidity increases when tested against alumina (Al_2O_3) aerosol. In addition, Durham and Harington[17] found that filter efficiency increases with increasing humidity for different filter fibers when challenged with fly ash. The apparent contradictions in the effects of humidity on filter efficiency require additional analysis to provide an assessment when respirators are used in high humidity workplaces.

Additional research on respirator performance is needed for several reasons. As mentioned above, human breathing consists of inhalation and exhalation airflow, not constant one-direction airflow as dictated in the NIOSH method for assessing FFRs' filtration performance.[5] Also, several studies that have simulated breathing to test the efficiency of FFRs did not take into account humidity in exhaled air.[7,9,18] Knowing the effects of air humidity upstream and downstream of a FFR is an important factor for improving FFR design and for a more efficient protection of workers who are exposed to particulates in high humidity workplaces. The goal of this study was to determine the effect of air temperature and humidity on the BR and particle penetration of N95 FFRs. The effect of air humidity on the BR was evaluated using a novel cyclic flow system. The effect of changes to the most penetrating particle size (MPPS) and the amount of mass gained of the FFRs were also characterized. Also, BR, water retention and moisture regain evaluations of individual FFR layers were performed.

Figure 1. Image of FFRs used in this study.

Methods

Filtering facepiece respirators (FFRs) characteristics

Two models of N95 respirators were selected for use in this study because they are commonly used in occupational settings and have different physical characteristics that could make them perform differently across temperature and relative humidity conditions (Figure 1). FFR 1 (3M 8510, St. Paul, MN) was a three-layer respirator with a rigid external layer followed by a middle layer of electret filter material and a thin internal layer. FFR 2 (Moldex 2200, Culver City, CA) was a two-layer respirator with a flexible mesh over the external electret filter material followed by a thin internal layer similar to that of FFR 1. Table 1 summarizes the physical characteristics of the tested FFRs. The filters were weighed in a balance with a sensitivity of 1 mg (Mettler PE 360, Mettler-Toledo LLC, Columbus, OH). The thickness of each layer was measured using a digital caliper (Neiko 01407A, Gardena, CA). Scanning electron microscopy (SEM) (Hitachi S-4800, Hitachi High Technologies America, Inc., Schaumburg, IL) of the FFRs were used to analyze fiber diameter. Fiber diameter and surface area were measured using ImageJ software (National Institutes of Health (NIH), Bethesda, MD). The method described by Balazy et al.[19] was used to calculate packing density (α).

Test system

Two test systems were designed to measure FFR particle penetration and BR under cyclic flow. Figure 2 shows the experimental setup used for measuring particle penetration and Figure 3 shows the experimental setup used for measuring BR. A plastic manikin head was used to

Table 1. FFRs characteristics (Mean ± S. D.).

FFR Model	Mass (g)	Thickness (mm)	Fiber diameter (µm)	Surface area (m^2)	Surface density ($g\ m^{-2}$)	Packing density (α)
FFR 1				0.0163		
External layer	3.53 ± 0.12	2.27 ± 0.28	22.1 ± 5.3		217.30	0.104
Middle layer	2.54 ± 0.17	1.77 ± 0.05	5.4 ± 3.2		156.11	0.096
Internal layer	0.55 ± 0.03	0.36 ± 0.08	15.4 ± 1.3		33.55	0.101
FFR 2				0.0188		
External layer	1.19 ± 0.01	1.30 ± 0.19	5.1 ± 4.6		63.01	0.053
Internal layer	0.53 ± 0.02	0.61 ± 0.11	15.5 ± 1.2		28.33	0.051

hold the FFR while performing both the particle penetration and BR tests. The manikin head was placed in a cubic acrylic plastic, sealed chamber with 38 cm sides (0.055 m^3). This chamber size was chosen to adequately contain the manikin head with an attached FFR and a mixing fan while minimizing aerosol spatial variability that may occur in a larger volume. As shown in Figure 2, the manikin head contained a pipe protruding from the mouth area to the back of the head to measure the aerosol concentration downstream of the FFR. This sample tube was contained within a larger pipe connected to a vacuum pump used to pull the main airstream through the FFR. A second sample tube protruded from the neck area of the manikin with an opening 12 cm from the first sample tube to sample aerosol concentration upstream of the FFR. A test was performed without a FFR attached to the manikin to verify that downstream counts were not different from upstream counts that might have been caused by the distance between the two sample pipe inlets and, therefore, the fan adequately mixed the aerosol within the chamber.

The breathing resistance test involved some components of the penetration test. As shown in Figure 3, a four-way connector was used to divide the airflow direction downstream of the FFR to create a cyclic flow pattern. A pipe connected a vacuum pump to one side of the four-way connector to pull air through the FFR and another pipe was used to connect an air pump to the other side of the four-way connector to push air through the FFR. Tubing from the available side of the four-way connector was attached to the same tube used to sample the downstream aerosol concentration during the penetration test to measure the downstream pressure. Likewise, the upstream

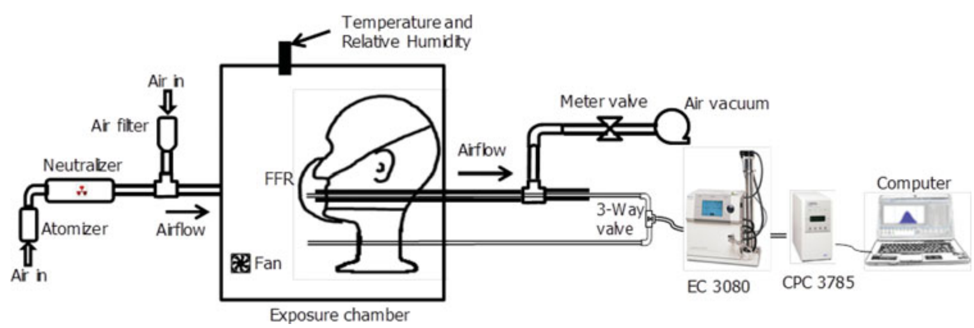

Figure 2. Schematic diagram of the test system used to determine NaCl particle penetration through an N95 FFR.

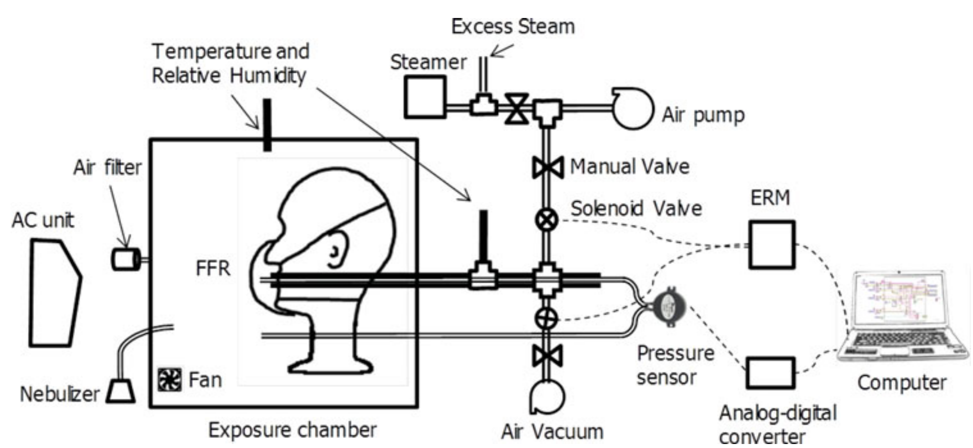

Figure 3. Experimental set up of the test system used to determine BR of an N95 FFR.

aerosol concentration tube was used to measure air pressure upstream of the FFR. Depending on the test, these two tubes were connected to a three-way valve (Figure 2) or to a differential pressure sensor (Figure 3). Air filters were connected to an inlet hole in the side of the chamber to remove particles from the make-up air that entered the chamber.

Particle penetration testing

Particle penetration was carried out in the chamber using a NaCl aerosol generated from a 2% solution applied to a nebulizer, as specified by NIOSH to certify N95 FFRs (42 CFR 84.181). The environmental conditions during both particle penetration tests (initial and final) were maintained at 25°C (77°F) and 30% relative humidity. The aerosol was charge-equilibrated with an ^{85}Kr source (Model 3077A, TSI Inc., St. Paul, MN). The generated aerosol passed through the charge equilibrator, was diluted with filtered air, and was sent to the inside of the chamber to generate a steady-state concentration (Figure 2). Aerosol generation was started and allowed to stabilize for 5 min. The penetration test required a continuous airflow of 85 L/min pulled through the FFR with a vacuum pump. A flowmeter (Model RMC-104, Dwyer Instrument Inc., Michigan City, IN) and a metered valve were placed between the chamber and the vacuum pump to establish the operational airflow. Airflow calibration was conducted with a primary calibrator (Model 4046, TSI Inc., Shoreview, MN) before each test.

The particle count and size distribution were measured with a scanning mobility particle sizer (SMPS) consisting of an electrostatic classifier (Model 3080, TSI Inc., Shoreview, MN) in combination with a condensation particle counter (CPC) (Model 3785, TSI Inc., Shoreview, MN). The SMPS counted particles within 103 channels ranging between 7–289 nm. As shown in Figure 2, the sample line to the SMPS was evenly split to enable sampling of particles upstream and downstream in the central portion of the FFR. A valve was manually turned to direct flow from one sample line to the other. The particle penetration was determined as a ratio of the particle concentration inside (C_{in}) the FFR and outside (C_{out}) the FFR for every SMPS size channel:

$$P\,(\%) = \frac{C_{in}}{C_{out}} \times 100. \tag{1}$$

During each trial, particle concentrations by size were measured with the SMPS three times in succession upstream of the FFR, then three times downstream of the FFR, and then again three times outside the FFR. C_{in} was calculated as the average of three measurements downstream of the FFR and C_{out} was the average of six measurements upstream of the FFR. The second set of upstream measurements were taken to ensure the aerosol concentration remained steady during each test; if the average of the two upstream aerosol measurements varied by more than 10%, that trial was rejected and re-conducted.[19] Given an average penetration for all size channels, the maximum penetration was obtained as well as the median diameter of the channel containing the maximum penetration, reported as the MPPS for the FFR under the tested conditions.

Breathing resistance testing

FFR BR was evaluated using cyclic flow and the experimental set-up shown in Figure 3. Inflowing air was conditioned to achieve 95% relative humidity and 36.7°C (98°F) to represent *exhaled air* from the inside to the outside of the FFR. A commercial steamer (Wagner 705, Plymouth, MN) supplied with distilled water was used to achieve both of these exhaled air conditions by producing warm, moist air that was controlled by venting a majority of the flow from the steamer, which was outside the chamber (Figure 3). Temperature and relative humidity were monitored with a factory calibrated environmental sensor (Q-Trak, TSI, Shoreview, MN) placed in an adapter in the pipe carrying the conditioned air through the manikin head to the inside space of the FFR.

To simulate inhaled air, a vacuum pump pulled air from upstream to downstream of the FFR at 55 L/min, a flow rate considered to be heavy breathing by workers. Airflow changes, between inhalation and exhalation occurred every 1.25 s (respiratory rate of 24 breaths/min) by periodically activating solenoid valves (DS6013, Burkert Inc., Irvine, CA; AVS-312-120A, Nitra Pneumatics, Cumming, GA). The minute volume of 55 L/min and breathing frequency of 24 breaths/min result in a tidal volume of 2.3 L, which is representative of lung conditions for males under a 60% pulmonary work rate.[20] The solenoid valves were connected to an electromechanical relay module connected to a computer. The LabVIEW (Ver. 2010, National Instruments, Chicago, IL) software program was used to operate the solenoid valves to switch between inhalation and exhalation modes while maintaining the airflow at 55 L/min.

Environmental conditions for inhaled air were varied. As shown in Table 2, simulated exhaled air conditions were compared to a control scenario in which both inhaled and exhaled air were set to room conditions (21.1°C (70°F), 40% RH). Inhaled air was conditioned with a combination of a portable air conditioner (AC) unit (PH3-12R-03, Soleus International Inc., City of Industry,

Table 2. Designed conditions during BR test (Mean ± S. D.).

	Inhalation		Exhalation	
Condition	T (°C)	RH (%)	T (°C)	RH (%)
0	22.4 ± 1.0	38.9 ± 3.9	22.4 ± 1.0	38.9 ± 3.9
1	25.1 ± 1.7	48.4 ± 9.3	34.5 ± 2.4	94.4 ± 5.3
2	15.4 ± 1.5	97.2 ± 2.7	34.9 ± 1.9	97.0 ± 4.3
3	17.7 ± 2.5	99.3 ± 1.8	34.4 ± 2.8	97.1 ± 3.2

CA) and a commercial nebulizer (Ultra-Neb 99, DeVilbiss Healthcare LLC, Somerset, PA). Distilled water was used in the nebulizer to produce moist air outside the filter as shown in Figure 3 and the AC unit produced an air temperature below room conditions (10°C (50°F)). The air inside the chamber was monitored with the Q-Trak protruding through a port in the top of the chamber.

A calibrated differential pressure sensor (Series 646B, Dwyer Instruments Inc., Michigan City, IN) measured BR across the FFR. As shown in Figure 3, the sensor was connected with tubing upstream and downstream of the central portion of the FFR. The pressure sensor range was 0–63.5 mm H_2O (0–2.5 in H_2O) via proportional voltage output of 0.5–4.5 V and was connected to an analog-to-digital converter to measure the voltage with a full scale accuracy of ±2%. During each trial, an initial BR measurement was made during the first minute of operation and then every 30 min over the 120-min trial period. During each measurement, the switching mechanism was stopped and BR was measured every 1 sec for 5 sec while operating with inhalation flow only of 55 L/min and an average computed for the five measurements taken.

Experimental design

Tests were conducted to determine how air humidity affects FFR particle penetration and BR under cyclic flow and various simulated air conditions. In general, FFRs were weighed before being sealed onto the manikin head. FFRs were sealed by firmly pressing two layers of 6-mm diameter rope caulk between the FFRs' border and the manikin head. Then, an initial NaCl aerosol penetration test was performed following NIOSH certification protocol (42 CFR 84.181) modified to not include preconditioning the FFR. Prior to obtaining measurements, and while the airflow through the FFR was 85 L/min, the pressure drop (BR) across the FFR was measured to test for leakage. Leakage was assumed if pressure drop < 5 mm H_2O and the trial terminated to reseal the FFR. Next, a BR test under cyclic flow was performed for 120 min and under a specific set of environmental conditions as shown in Table 2. Conditions were tested always in order from Condition 0 to Condition 3, for 5 individual FFRs per condition. After 120 min, a second ("final") NaCl aerosol penetration test was performed. Finally, the FFR was removed from the manikin head and reweighed. The difference between initial and final weight was referred to as the mass gained (MG).

Condition 0 served as a control environment consisting of typical room temperature and relative humidity for both the inhalation and exhalation air. Condition 1 was a modification of Condition 0 by simulating human exhaled breath consisting of air at 36.7°C (98°F) and 95% RH.[15] Condition 2 was a modification of Condition 1 to include cool, humid inhalation air to simulate situations that may enhance water absorption by the filter media. Condition 3 was similar to Condition 2 except the humidity was increased just to the point of saturation (100% RH) to simulate conditions when condensation may occur. Five trials per simulated condition per FFR were completed.

Evaluation of unused FFR individual layers

Since the tested N95 FFRs were multilayered, FFR layers were tested individually to evaluate BR, water retention value (WRV) and moisture regain value (MRV) by layer. It was of interest to us to determine differences at the filter layer level primarily with regard to BR. The WRV provides an indication of the amount of moisture absorbed into, and retained within, the filter fibers.[21] The MRV is a measure of the moisture that is adsorbed on the surface of the filter fibers.[23] SEM images were also obtained to examine the composition of the FFRs external layers visually.

BR of individual FFR layer

BR of unused, unexposed FFR individual layers were measured by first cutting out a section of the filter layer and passing air with 95% RH through the layer using a constant flow equivalent to 55 L/min. A device was developed for this purpose that consisted of a stainless-steel Tri-Clover clamp apparatus. This apparatus consisted of two 3.8-cm diameter flat circular pieces with a 1.6 cm diameter central hole that were clamped together to hold a 2.5-cm diameter piece of filter layer securely while air flowed through the center hole and through the area of the filter layer covering the hole. Pressure taps were applied on either side of the clamp apparatus to measure BR for 30 min in triplicate.

Water retention value

The WRV of each filter layer was determined following the methods described by Siroka et al.[21] and Kongdee et al.[22] Filter layer sections were immersed in deionized water at room temperature for 24 hr. Then, the filter layer sections were centrifuged at 4000 g for 10 min to remove excess water and weighed (W_w) in a microbalance. The filter layer sections were then dried in an oven at 105°C for 4 hr, and reweighed (W_d). WRV was calculated using the following equation:

$$WRV = \frac{W_w - W_d}{W_d}. \quad (2)$$

Moisture regain value

The MRV of each filter layer was determined following the method described in Kongdee et al.[22] Filter layer sections were conditioned in a standard atmosphere of 85% RH at room temperature for 48 hr and then weighed (W_C). The sections were then dried in an oven at 105°C for 4 hr and reweighed (W_D). MRV was calculated using the following equation:

$$MRV = \frac{W_C - W_D}{W_D}. \quad (3)$$

Statistical analysis

Two statistical analyses were performed to assess differences in the means of the variables MPPS, percent penetration, BR, and MG within FFRs. The first analysis compared initial and final means within FFRs. The second analysis was conducted to determine differences between the means of each variable determined under Condition 0, as the control condition, and Conditions 1, 2, and 3 as defined in Table 2. All comparisons were conducted as two-sample T-tests. A third analysis involved a one-way ANOVA followed by a Tukey's pairwise comparison to compare the means of the differences in the initial-to-final BR obtained between conditions for each FFR. Statistical analyses were performed with Minitab® (Ver. 17, Minitab Inc., State College, PA). Statistical significance was accepted at the $\alpha = 0.05$ level.

Results

Data sets were tested for normality using the Anderson-Darling test and found to be normally distributed. The mean initial and final values of the 20 total samples independent of environmental condition are presented in Table 3. Data is separated to compare both within and between FFRs. Table 4 provides results separated by test condition. Displayed are the mean values for the five samples taken for each condition at the end of each trial.

Table 3. Initial and final means and standard deviations of most penetrating particle size (MPPS), penetration (P), breathing resistance (BR), and FFR mass for all conditions combined.

	MPPS, nm	P, %	BR, mm H_2O	Mass, g
FFR 1 Initial	41.7 ± 4.7	2.8 ± 0.7	11.2 ± 0.8	10.6 ± 0.2
FFR 1 Final	43.5 ± 3.8	3.1 ± 1.1	**13.1** ± 1.8	**12.0** ± 1.2
FFR 2 Initial	50.5 ± 5.4	5.1 ± 1.6	13.0 ± 0.8	14.2 ± 0.4
FFR 2 Final	52.4 ± 7.6	5.3 ± 2.0	**16.8** ± 3.3	**15.8** ± 1.4

Bolded values are significantly different ($\alpha < 0.05$) from the comparable initial value.

Most penetrating particle size

The final mean MPPS values did not differ from the initial MPPS values within either FFR model [FFR 1 (p = 0.17) and FFR 2 (p = 0.16)]. Comparisons of the final MPPS (Table 4) between Condition 0 and all other conditions within FFR model were not significantly different for any condition.

Particle penetration

The mean penetration values for the FFR 1 were below the NIOSH certification limit. However, the mean penetration values obtained for FFR 2 exceeded the 5% NIOSH certification limit for two test conditions (Table 4).

Figure 4 shows the difference between the final and initial penetration measurements for the two FFRs for each simulated test condition. Aerosol penetration increased between the initial and final tests for all conditions for both FFRs except Condition 2 for FFR 1 and Condition 0 for FFR 2 (Figure 4). However, the average final mean penetration values (Table 3) for both FFR models did not differ significantly from the average initial penetration values within FFR model [FFR 1 (p = 0.34) and FFR 2 (p = 0.69)] (Table 4).

Comparisons of the final penetrations within FFR 2 and between conditions were significantly different

Table 4. Final values of the most penetrating particle size (MPPS), penetration (P), breathing resistance (BR), and mass gained (MG) for each respirator and each test condition (Mean ± S. D.).

	Test Conditions			
FFR models	0	1	2	3
FFR 1				
MPPS, nm	40.6 ± 2.5	43.0 ± 2.4	44.3 ± 3.0	46.3 ± 5.1
P, %	2.5 ± 0.9	2.9 ± 0.7	2.6 ± 0.2	4.2 ± 1.4
BR, mm H_2O	11.7 ± 1.0	13.5 ± 1.6	**14.3**[a] ± 1.6	13.0 ± 2.4
MG, g	0.003 ± 0.085	**1.05** ± 0.61	**1.74** ± 0.73	**2.82** ± 0.98
FFR 2				
MPPS, nm	54.0 ± 7.3	51.3 ± 11.1	49.1 ± 5.1	55.1 ± 6.5
P, %	3.8 ± 0.7	**7.2** ± 1.7	3.8 ± 0.4	**6.5** ± 1.7
BR, mm H_2O	13.5 ± 0.3	**15.0** ± 0.7	**17.1** ± 1.2	**21.6** ± 1.1
MG, g	0.059 ± 0.034	**1.44** ± 0.71	**2.05** ± 0.32	**2.84** ± 1.02

[a]Bolded values are significantly different ($\alpha < 0.05$) from comparable value obtained under Condition 0.

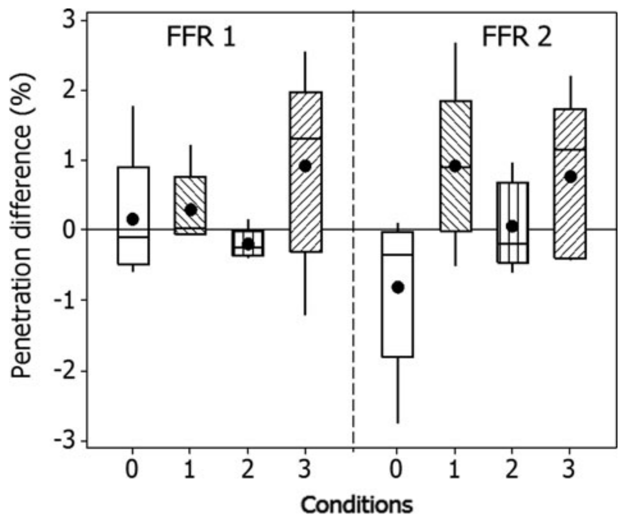

Figure 4. Difference in particle penetration for two N95 FFRs (n = 5 per condition). The boxplot whiskers represent the lowest and highest values measured; the box ranges from 25– 75% percentiles; the horizontal line is the median; and the black circle is the arithmetic mean.

between Condition 0 and Conditions 1 and 3 for FFR 2 (Table 4). The similar comparisons between conditions for FFR 1 did not result in significant differences.

Breathing resistance

The final mean BR values (Table 3) for both FFR models differ from and were greater than the initial BR values within FFR model ($p < 0.001$). Comparisons of BR within the FFRs and between conditions showed significant differences between Condition 0 and Condition 2 for FFR 1 and between Condition 0 and all other conditions for FFR 2 (Table 4).

After 120 min of testing, none of the FFR's exceeded the NIOSH certification limit for BR of 35 mm H_2O (Table 4). Given these results, the BR after an 8-hr work shift would be expected to be between 20–24 mm H_2O for FFR 1 and between 22–49 mm H_2O for FFR 2 between Conditions 1 and 3.

A box plot of the differences between the final and initial BR values for both FFRs tested for the four different simulated test conditions is given in Figure 5. Results from the one-way ANOVA analysis demonstrated significant differences between the means of the BR changes for each condition for both FFR 1 ($p = 0.010$) and FFR 2 ($p < 0.001$). Table 5 summarizes the mean differences in BR for each condition and provides the results from the Tukey's pairwise analysis performed to determine BR differences between conditions. Two similar groups were identified for FFR 1 and 3 groups for FFR 2.

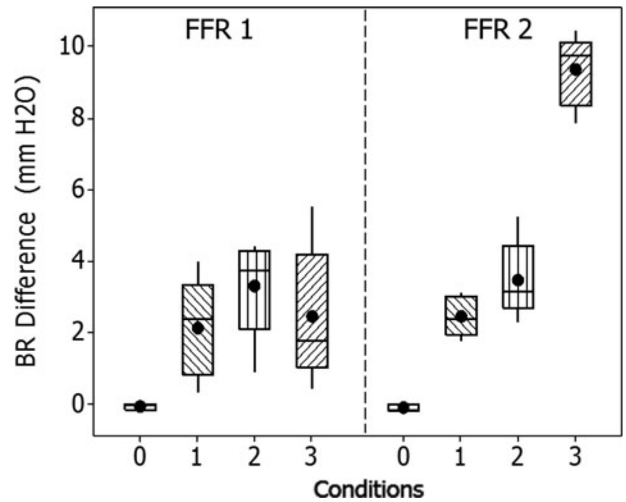

Figure 5. Difference in breathing resistance for two N95 FFRs (n = 5 per condition). Interpretation of the box plots is given in Figure 4.

Mass gained

The final mean mass values for both FFR models were greater than the initial mass values within FFR model ($p < 0.001$) (Table 3). Comparisons of MG within the FFRs and between conditions showed significant increase in moisture retention between Condition 0 and all other conditions for both FFRs (Table 4).

A box plot was constructed of the difference between the final and initial MG values for the two FFRs tested against the four different simulated air conditions (Figure 6). As shown in Figure 6, MG increased when the humidity in the air passing through the FFR increased for both FFR models.

Filter layers

The presence or absence of a change in BR generated by air humidity applied to filter layers for each FFR over 30 min is summarized in Table 6. BR increases were only observed on the middle layer for FFR 1 and on the external layer for FFR 2. WRV magnitude of change is also summarized on Table 6. A notable increase in WRV was only observed in the external layer of FFR 1. The magnitude of change in MRV is also summarized in Table 6,

Table 5. Means of differences in breathing resistance (BR) for each FFR (Mean ± S. D.).

	FFR 1		FFR 2	
Condition	BR	Group	BR	Group
0	− 0.1 ± 0.1	A	− 0.1 ± 0.1	A
1	2.1 ± 1.4	AB	2.5 ± 0.6	B
2	3.3 ± 1.4	B	3.5 ± 1.1	B
3	2.4 ± 1.9	B	9.3 ± 1.0	C

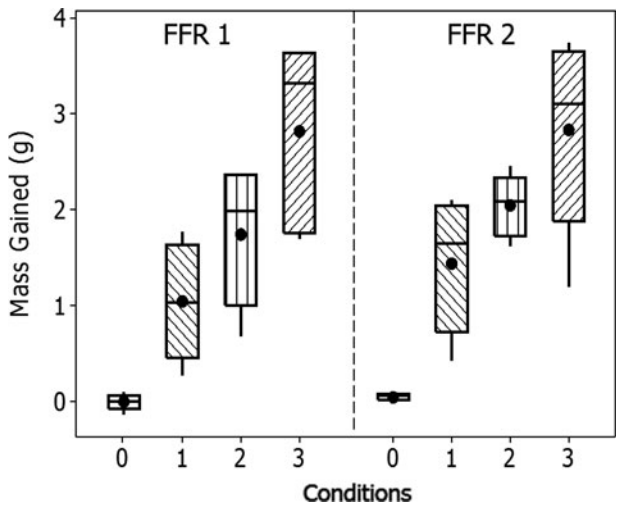

Figure 6. Mass gained for two N95 FFRs (n = 5 per condition) Interpretation of the box plots is given in Figure 4.

however, no change was observed on the MRV on the filter layers. Figure 7 shows SEM micrographs of all the filter layers examined in this study. As can been seen, the inner layer looks similar for both FFR. Similar physical features can also be seen on FFR 1 middle layer and FFR 2 external layer. However, the external layer of FFR 1 is comprised of a different filter media relative to all the other layers; the gaps between the fibers (filter porosity) are greater and fiber diameter is also bigger (Table 1).

Discussion

This study demonstrated that humid air passing through an FFR over time does not affect its particle capture capabilities. The efficiency of the FFRs tested during this study remained constant even in humid conditions in which the FFRs gained considerable moisture (Figure 6). Previous studies reported an increase or a decrease in particle penetration under humid conditions.[16,17] However, those studies both changed humidity levels and challenged the filters with a test aerosol (Al_2O_3 and fly ash) at the same time, so it cannot be determined whether humidity alone affected penetration from those studies. Motyl and Lowkis[23] demonstrated that humidity will degrade the charge on electret filter media, but that effect required over two weeks of continuous humidity exposure.

This study also demonstrated that the BR increased as humidity was applied to the FFRs over time. Since no aerosols were used during the BR test described here and distilled water was used to create the humidity in the air, we can assume that the increase in BR can be related to moisture absorbed within the fibers or adsorbed between fibers of the FFRs. The results for FFR 2 under Condition 3 indicate that the BR may exceed the NIOSH maximum of 35 mm H_2O if worn in that condition over an 8-hr work shift. This would necessitate the use of multiple FFRs over the work day.

Contal et al.[24] also demonstrated an increase in BR through filters associated with a clogging effect when loaded with non-aqueous liquid aerosols for which water may have a similar effect. However, Gupta et al.[25] exposed HEPA filters to both humidity and a test aerosol and stated that with increasing humidity in air, BR decreased on the filters. Gupta also indicated that these effects are postulated to be due to the effect of humidity on particle cake formation that results in creation of channels through which the air can flow with less resistance.

Our results showed a greater increase in BR than reported by Roberge et al.[12] who also performed a study involving FFR BR. This increase could be due to a different breathing rate during the cyclic flow and time selected to evaluate the BR. Our study evaluated BR at a heavy breathing rate, while Roberge et al.[12] evaluated the BR at a moderate breathing rate (40 L/min). The difference in breathing rate may have resulted in a different amount of humid air passing through the FFR and therefore accumulated a greater amount of moisture in the FFRs tested in this study.

As shown in Figure 6, both FFRs retained moisture compared to the test condition with an increase in MG with increased contact with high humidity air. An increase in MG was observed just by applying humidity to simulate human exhaled breath while "inhaling" room air conditions. As shown in Figure 5, an increase in BR was likewise observed under Condition 1 indicating that human breath associated with wearing an FFR will increase the BR of an FFR. This result indicates that

Table 6. Values in breathing resistance (BR), water retention value (WRV), and moisture regain value (MRV) for the individual layers of each FFR (Mean ± S. D.).

	FFR 1			FFR 2	
Parameters	Inner layer	Middle layer	External layer	Inner layer	External layer
BR	0.51 ± 0.04	3.63 ± 1.32	0.64 ± 0.05	0.21 ± 0.06	10.4 ± 1.61
WRV	0.030 ± 0.016	0.423 ± 0.037	4.71 ± 0.321	0.013 ± 0.028	0.105 ± 0.007
MRV	0.005 ± 0.002	0.002 ± 0.0003	0.003 ± 0.0003	0.0004 ± 0.001	0.002 ± 0.002

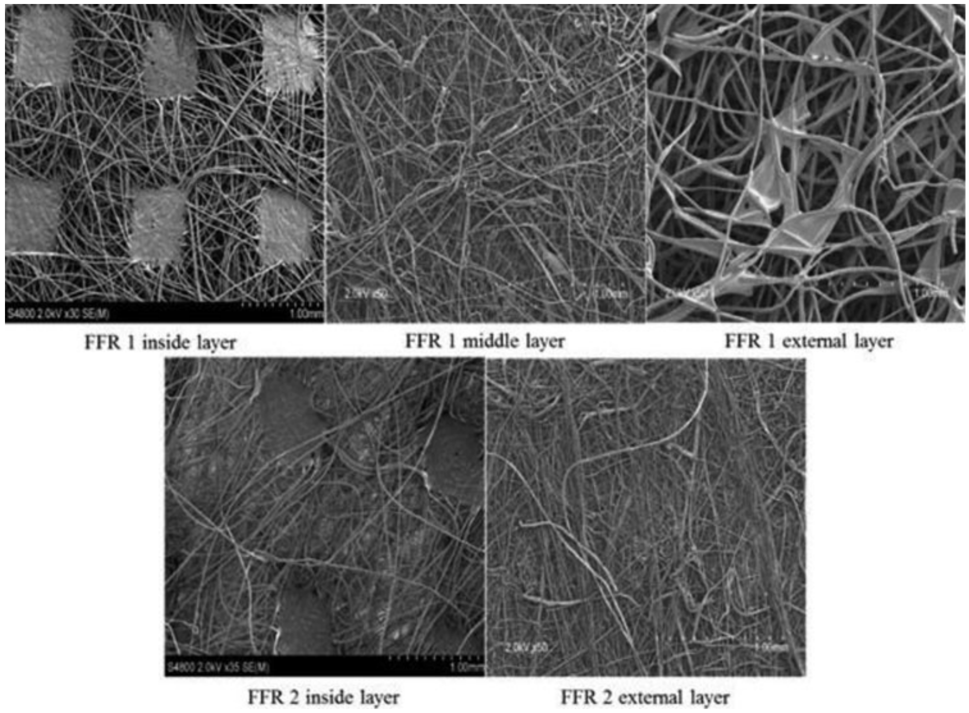

Figure 7. SEM of FFR individual layers (X30-50).

FFRs certified for BR under room air conditions underestimate the BR of an FFR as worn by a user by at least 2 mm H_2O for the FFRs tested. Given that an increase in BR will necessarily occur when worn suggests that theoretical equations to estimate BR, such as that given by Hinds,[26] should be adapted to include the effect of humidity. For example, Miguel[16] applied this effect in an overall model to estimate the pressure drop of fibrous filters affected by a range of humidity conditions.

Further increases in MG (Figure 6) for both FFRs resulted from additional humidity in the upstream air. However, as shown in Figure 5, when the FFRs were tested with high humidity in the upstream air (Conditions 2 and 3), the BR outcomes behave differently between the two FFRs. There was an increase in BR for FFR 1 in a range of 1–4 mm H_2O for both conditions. Whereas BR increased substantially in FFR 2 for Condition 3 with saturated air. An explanation for this effect may be related to the results given in Table 6. Those results show that the increase in BR resulting from exposure to humidity occurs primarily in the electret filter media layer (middle for FFR 1 and external for FFR 2). However, FFR 1 has an external support layer consisting of fiber media that resulted in a substantial change in the water retention value (WRV) under high humidity, which may therefore capture moisture before affecting the middle, electret layer. Furthermore, as shown in Figure 7, the gaps between fibers in the FFR 1 external layer are larger than those in any other layer. Kongdee et al.[22] provided evidence to show that larger filter gap size, or "pore volume", results in higher water retention between the gaps.

There were some limitations of this work. The device used to measure relative humidity provided measurements in the range of 0–100% but was most accurate up to a reading of 95%. Therefore, the relative humidity of the atmosphere created in the test system was in the upper limit of accuracy of that instrument. Furthermore, even though FFRs were sealed and were tested for leakage at high airflow, there may be a possibility that a small leakage would be unnoticed by our testing method. Only one breathing pattern was simulated in this study, therefore, further studies are needed to address the issue of the effect of humidity in air given multiple breathing patterns on FFRs performance.

Conclusions

Two NIOSH certified N95 FFRs were tested against four different simulated temperature and humid air conditions in a laboratory setting. Results from this study demonstrated that particle penetration was not affected by high humidity. The FFRs, therefore, retained their capabilities as a certified respiratory device when subjected to the tested environmental conditions. Furthermore, high humidity in exhalation air, in inhalation air, or both, increases BR through FFRs. The high porosity external layer of FFR 1 mitigated this effect. Therefore, tasks carried out in high humidity environments may require an evaluation of different FFRs to determine which is less effected by humidity, or reduce the time that an FFR is used by a worker.

Acknowledgments

We express their thanks to Dr. Nathan Fethke and Ralph Altmaier, The University of Iowa Department of Occupational & Environmental Health, for their expertise and assistance with planning this study.

Funding

This research was supported (in part) by a pilot project research training grant from the Heartland Center for Occupational Health and Safety at the University of Iowa. The Heartland Center is supported by Training Grant No. T42OH008491 from the Centers for Disease Control and Prevention/National Institute for Occupational Safety and Health.

References

[1] "Standard for Respiratory Protective Devices," *Code of Federal Regulations Title 42*, Part 84. 1995. pp. 546–549.
[2] **Doney, B.C., D.W. Groce, D.L. Campbell, et al.:** A survey of private sector respirator use in the United States: an overview of findings. *J. Occup. Environ. Hyg.* 267–276 (2005).
[3] **Occupational Safety and Health Administration (OSHA):** "United States Department of Labor. Respiratory Protection." Available at https://www.osha.gov/SLTC/respiratoryprotection/index.html (accessed January , 2015).
[4] **Friedlander, S.:** Theory of aerosol filtration. *Aerosol Filtrat.* 1161–1164 (1958).
[5] **National Institute for Occupational Safety and Health (NIOSH):** *Determination of Exhalation Resistance Test, Air Purifying Respirators Standard Testing Procedure* Pittsburgh. (2005).
[6] **Johnson, A.:** How much work is expended for respirator? *Front. Med. Biol. Eng.* 265–287 (1993).
[7] **Cho, K., T. Reponen, R. McKay, R. Shukla, H. Haruta, and P. Sekar:** Large particle penetration through N95 respirators filters and faceseal leaks with cyclic flow. *Ann. Occup. Hyg.* 68–77 (2010).
[8] **Cho, K., L. Turkevich, M. Miller, R. McKay, S. Grinshpun, and K. Ha:** Penetration of fibers versus spherical particles through filter media and faceseal leakage of n95 filtering facepiece respirators with cyclic flow. *J. Occup. Environ. Hyg.* 109–115 (2013).
[9] **Eshbaugh, J.P., P.D. Gardner, A.W. Richarson, and K.C. Hofrace:** N95 and P100 respirator filter efficiency under high constant and cyclic flow. *J. Occup. Environ. Hyg.* 52–61 (2009).
[10] **Grinshpun, S., H. Haruta, R. Eninger, T. Reponen, R. McKay, and S. Lee:** Performance of an N95 filtering face-piece particulate respirator and a surgical masks during human breathing: two pathways for particle penetration. *J. Occup. Environ. Hyg.* 593–603 (2009).
[11] **Janssen, L.:** Efficiency and pressure drop effects of high concentrations of cement dust on N95 electret filters. *J. Int. Soc. Respir. Protect.* 75–82 (2004).
[12] **Roberge, R., E. Bayer, J. Powell, A. Coca, M. Roberge, and S. Benson:** Effect of exhaled moisture on breathing resistance of N95 filtering facepiece respirators. *Ann. Occup. Hyg.* 671–677 (2010).
[13] **Cho, H.W., C.S. Yoon, J.H. Lee, S.J. Lee, A. Viner, and E. Johnson:** Comparison of pressure drop and filtration efficiency of particulate respirators using welding fumes and sodium chloride. *Ann. Occup. Hyg.* 666–680 (2011).
[14] **Cho, H., and C. Yoon:** Workplace field testing of the pressure drop of particulate respirators using welding fumes. *Ann. Occup. Hyg.* 948–958 (2012).
[15] **Shaviv, N:** "Science Bits." Available at http://www.sciencebits.com/ExhaleCondCalc?calc=yes (accessed March , 2013).
[16] **Miguel, A.:** Effect of air humidity on the evolution of permeability and performnce of a fibrous filter during loading with hygroscopic and non-hygroscopic particles. *J. Aerosol Sci.* 783–799 (2003).
[17] **Durham, J., and R. Harrington:** Influence of relative humidity on filtration resistance and efficiency of fabric dust filters. *Filtr. Separ.* 389–398 (1971).
[18] **Rengasamy, S., and B.C. Eimer:** Total inward leakage of nanoparticles through filtering facepiece respirators. *Ann. Occup. Hyg.* 253–263 (2011).
[19] **Balazy, A., M. Toivola, T. Reponen, A. Podgoeski, A. Zimmer, and S. Grinshpun:** Manikin-based performance evaluation of N95 filtering-facepiece respirators challenged with nanoparticles. *Ann. Occup. Hyg.* 259–269 (2006).
[20] **Janssen, L.L., N.J. Anderson, P.E. Cassidy, R.A. Weber, and T.J. Nelson:** Interpretation of inhalation airflow measurements for respirator design and testing. *J. Int. Soc. Respir. Protect.* 122–141 (2005).
[21] **Siroka, B., M. Noisternig, U.J. Griesser, and T. Bechtold:** Characterization of cellulosic fibers and fabrics by sorption/desorption. *Carb. Res.* 2194–2199 (2008).
[22] **Kongdee, A., T. Bechtold, E. Burtscher, and M. Scheinecker:** The influence of wet/dry treatment on pore structure-the correlation of pore parameters, water retention and moisture regain values. *Carb. Polym.* 39–44 (2004).
[23] **Motyl, E., and B. Lowkis:** Effect of air humidity on charge decay and lifetime of PP electret nonwovens. *Fib. Text.* 39–42 (2006).
[24] **Contal, P., J. Simao, D. Thomas, et al.:** Clogging of fibre filters by submicron droplets. Phenomena and influence of operating conditions. *Aerosol Sci.* 263–278 (2004).
[25] **Gupta, A., V. Novick, P. Biswas, and P. Monson:** Effect of humidity and hygroscopicity on the mass loading capacity of high efficiency particulate air (HEPA) filter. *Aerosol Sci. Technol.* 94–107 (1993).
[26] **Hinds, W.:** *Aerosol Technology* New York: Wiley Interscience Publication, 1999. pp. 182–205.